TISSUE ENGINEERING: Part A
Volume 20, Numbers 21 and 22, 2014

DOI: 10.1089/ten.tea.2012.0726

Improvement of Bone Regeneration Capability of Ceramic Scaffolds by Accelerated Release of Their Calcium Ions

Young-Joon Seol, PhD,[1] Ju Young Park, MS,[2] Jin Woo Jung, BS,[3] Jinah Jang, BS,[2] Rijal Girdhari, PhD,[3] Sung Won Kim, MD, PhD,[4] and Dong-Woo Cho, PhD[3]

To regenerate the bone tissue, the fabrication of scaffolds for better tissue regeneration has attracted a great deal of attention. In fact, growth factors are already used in clinical practice and are being investigated for enhancing the capacity for bone tissue regeneration. However, despite their strong osteoinductive activity, these growth factors have several limitations: safety issues, high treatment costs, and the potential for ectopic bone formation. The aim of this study was therefore to develop ceramic scaffolds that could promote the capacity for bone regeneration without growth factors. Three-dimensional ceramic scaffolds were successfully fabricated from hydroxyapatite (HA) and tricalcium phosphate (TCP) using projection-based microstereolithography, which is an additive manufacturing technology. The effects of calcium ions released from ceramic scaffolds on osteogenic differentiation and bone regeneration were evaluated *in vitro* and *in vivo*. The osteogenesis-related gene expression and area of new bone formation in the HA/TCP scaffolds was higher than those in the HA scaffolds. Moreover, regenerated bone tissue in HA/TCP scaffolds were more matured than that in HA scaffolds. Through this study, we were able to enhance the bone regeneration capacity of scaffolds not by growth factors but by calcium ions released from the scaffolds. Ceramic scaffolds developed in this study might be useful for enhancing the capacity for regeneration in complex bone defects.

Introduction

Bone is a dynamic living tissue, and is built and resorbed by osteocytes, osteoblasts, and osteoclasts. The fracture of bone activates osteogenesis and it heals itself without any treatment.[1] Although bone tissue has its own capacity to regenerate, this ability is limited to small bone defects. In the case of large bone defects, graft implantations such as autografts and allografts have been widely used in clinical practice. Autografts, in particular, have been considered the gold standard bone grafting material. However, they have many drawbacks such as the additional surgery required to obtain the graft material, infection at the host graft site, and limited graft material supply.[2,3] To address these issues, tissue engineering has been introduced,[4,5] and the fabrication of scaffolds for better tissue regeneration has attracted a great deal of attention because commonly used materials for scaffolds such as polycaprolactone (PCL) and poly(lactic-*co*-glycolic acid) (PLGA) have a lower capacity for osteogenesis than the materials of graft implantation.

A number of key molecules that are able to induce osteogenesis have been identified, which are already used in clinical practice and are under investigation to enhance the capacity for bone tissue regeneration.[6–8] They are growth factors such as bone morphogenic protein, fibroblast growth factor, vascular endothelial growth factor, and insulin-like growth factor, and they have been loaded in scaffolds to enhance bone regeneration. However, despite their strong osteoinductive activity, these molecules have several limitations: safety issues, high treatment costs, and the potential for ectopic bone formation.[9,10] It has been reported that not only growth factors but also calcium ions play a role in inducing bone formation in bone tissue regeneration. Calcium ions activate the chemotaxis of osteoblasts and osteogenic differentiation of stem cells, and stimulate osteoclasts to release growth factors.[8,11–15] Among the materials for bone tissue scaffolds, calcium phosphate ceramics, hydroxyapatite [HA: $Ca_{10}(PO_4)_6(OH)_2$], and tricalcium phosphate [TCP: $Ca_3(PO_4)_2$], which are the inorganic components of native bone tissue, release calcium ions during degradation. Moreover, these materials also have biocompatibility

[1]Wake Forest Institute for Regenerative Medicine, Wake Forest School of Medicine, Winston-Salem, North Carolina.
[2]Division of Integrative Biosciences and Biotechnology, Pohang University of Science and Technology (POSTECH), Pohang, Korea.
[3]Department of Mechanical Engineering, Center for Rapid Prototyping Based 3D Tissue/Organ Printing, Pohang University of Science and Technology (POSTECH), Pohang, Korea.
[4]Department of Otolaryngology-Head and Neck Surgery, College of Medicine, The Catholic University of Korea, Seoul, Korea.

and osteoconductivity; thus, they are excellent materials for bone tissue regeneration.[16–18]

Until now, most scaffolds for regenerating tissue in bone defects have been fabricated by traditional methods such as particulate leaching, gas foaming, and phase separation. However, it is difficult to control the pore size and shape with full interconnectivity, and to fabricate scaffolds adapted for improved cell growth and tissue regeneration.[19–21] To overcome these limitations of the traditional manufacturing methods, recent attempts have been directed to fabricating scaffolds using computer-aided design and computer-aided manufacturing. These attempts are additive manufacturing (AM) technologies, and they can fabricate scaffolds with customized and predefined inner and outer shapes.[21–26]

The aim of this study was therefore to develop ceramic scaffolds that were able to promote the capacity for bone regeneration without growth factors using AM technology. The ceramic scaffolds were fabricated from HA and TCP powders, and the quantity of calcium ions released from the ceramic scaffolds was controlled by the composition of HA and TCP. The effects of calcium ions on bone regeneration were evaluated by *in vitro* and *in vivo* experiments.

Materials and Methods

Ethics statement

In this study, the experimental procedures were approved by the Institutional Review Board of Seoul St. Mary's Hospital Catholic University of Korea and POSTECH. All of the patients provided written informed consent for the collection of cells and subsequent evaluation.

Preparation of materials

Commercially available ceramic powders, HA and TCP (Berkeley Advanced Biomaterials, Berkeley, CA) with 100 nm in diameter, were used to fabricate the ceramic scaffolds for bone tissue. Because these materials alone are not photocurable, we prepared a slurry mixture of ceramic powder with photocurable resin (FA1260T; SK-Cytec, Seoul, Korea). To determine the effects of calcium ions, we prepared the HA and HA/TCP (7:3 wt%) powder. A 20% volume ratio of ceramic powder to photocurable resin was used to maintain sufficient fluidity, and the weight of HA and TCP were calculated using densities of 3.185 and 3.016 g/cm^3, respectively. In the *in vivo* experiment, commercialized HA ceramic scaffolds (BABI-HAP-PD; Berkeley Advanced Biomaterials) fabricated by traditional methods were used for comparison with ceramic scaffolds fabricated by AM technology.

Fabrication of ceramic scaffolds

Projection-based microstereolithography (pMSTL) and sintering were used to fabricate the ceramic scaffolds (HA and HA/TCP scaffold). The cuboid ceramic scaffolds of $4 \times 4 \times 3$ mm were designed for *in vitro* experiments, and the cylindrical scaffolds of 8 mm in diameter and 1.5 mm in height were designed for the *in vivo* experiments. The desired 3D structures were fabricated by the pMSTL system with a 450 W UV lamp. The 3D structures then were immersed in acetone for 10 min, and air was blown through them to remove any unsolidified resin in the structures. After fabrication, sintering followed to cause the ceramic particles to adhere to one another and to remove the solidified photocurable resin. The temperature was increased to 1400°C at a heating rate of 5°C/min in ambient air using a furnace (LTF 15/50/180; Lenton, Hope Valley, Derbyshire, United Kingdom). The maximum temperature was maintained for 2 h to provide sufficient energy for sintering.

Calcium ion release test

The quantity of calcium ions released from the ceramic scaffolds was determined using a calcium colorimetric assay kit (Cat. K380-250; BioVision, Milpitas, CA). Ceramic scaffolds were individually immersed into 1 mL cell culture medium (α-minimum essential medium [α-MEM] supplemented with 10% fetal bovine serum [FBS], 100 U/mL penicillin, and 100 μg/mL streptomycin) at 37°C under static condition. The supernatants were taken from the solution every 2 days to maintain a constant calcium ion concentration. The supernatants were mixed with chromogenic reagent and calcium assay buffer and incubated for 10 min at room temperature in darkness; then, their optical densities were measured at 575 nm. These measurements were collected every second day for 2 weeks. Cell culture medium without a ceramic scaffold was used as a control.

In vitro *experiments*

Biocompatibility test. To assess the biocompatibility of fabricated ceramic scaffolds, a cell proliferation test was performed. Human turbinate mesenchymal stromal cells (hTMSCs), which were isolated from inferior turbinate tissue, were cultured in α-MEM supplemented with 10% FBS, 100 U/mL penicillin, and 100 μg/mL streptomycin at 37°C in a humidified atmosphere of 5% CO_2, and the medium was changed every 3 days. After subculture, the cells were harvested with trypsin-ethylenediaminetetraacetic acid (EDTA) and aliquots of 1×0^4 cells were seeded onto each scaffold (HA and HA/TCP scaffolds). The scaffolds were cultured in medium for 14 days. On days 1, 3, 7, and 14, the quantity of DNA in the cells was evaluated to determine the biocompatibility of the scaffolds.

Alizarin Red-S staining. Alizarin Red-S (AR-S) staining was used to analyze calcium precipitation after 14 days of culture in normal medium and osteogenic medium. After removing the medium, the scaffolds and cells were gently washed with phosphate-buffered saline (PBS) and fixed in 10% formalin for 12 h at room temperature. They were washed with distilled water and stained with AR-S solution for 5 min in the dark. They were then washed with PBS for 24 h to perfectly remove the excess staining solution, and the stained solution was extracted using EDTA. The absorbance at 590 nm was measured using a microplate reader to quantify the calcium precipitation.

Real-time reverse transcription–polymerase chain reaction. The cell differentiation was evaluated using reverse transcription–polymerase chain reaction (RT-PCR) to evaluate the gene expression of cells in the ceramic scaffolds. After cell culture on different ceramic scaffolds for 14 days in normal medium and osteogenic medium, total RNA was isolated using TRIzol (Invitrogen, Groningen, Netherlands)

according to the manufacturer's protocol; then cDNA was synthesized using isolated RNA and the superscript first-strand synthesis system (Invitrogen). To evaluate the expression of osteogenic markers such as osteocalcin (*OCN*), runt-related transcription factor 2 (*Runx2*), and collagen type I (*Col-I*), SYBR Green PCR Master Mix (Applied Biosystems, Warrington, United Kingdom) assay was used to perform real-time quantitative RT-PCR. The expression values of the osteogenic markers were normalized to that of glyceraldehyde-3-phosphate dehydrogenase (*GAPDH*). The following primers were used: *GAPDH* sense, 5′-CCAGG TGGTCTCCTCTGACTTC-3′; *GAPDH* antisense, 5′-GTG GTCGTTGAGGGCAATG-3′; *OCN* sense, 5′-GTGCAGA GTCCAGCAAAGGT-3′; *OCN* antisense, 5′-TCAGCCAA CTCGTCACAGTC-3′; *Runx2* sense, 5′-AACCCACGAAT GCACTATCCA-3′; *Runx2* antisense, 5′-CGGACATACC GAGGGACATG-3′; *Col-I* sense, 5′-CTGCAAGAACAGC ATTGCAT-3′; and *Col-I* antisense, 5′-GGCGTGATGGC TTATTTGTT-3′.

In vivo *experiment*

Implantation of ceramic scaffolds. The *in vivo* experiment was performed on male Sprague-Dawley rats (12-week-old, average weight 300–350 g) based on a rat calvarial defect model. Routine antibiotics were prescribed preoperatively to prevent infection, and general anesthesia was induced with 50 mg/kg of ketamine (Yuhan Co., Seoul, Korea) and 3 mg/kg of xylazine (Bayer Korea Ltd., Seoul, Korea). The calvarial defects, 8 mm in diameter, were created in the central part of the calvarial bone using a trephine bur without dura perforation. Commercialized BABI-HAP-PD scaffolds, HA scaffolds, and HA/TCP scaffolds were then placed in the calvarial defects without cells. Rats with no defect treatment were used as negative controls. Each experimental group contained five rats, and they were sacrificed at the 16th week after implantation. The extraction samples were fixed with 10% formaldehyde solution for evaluation.

Evaluation of *in vivo* experimental results. To visualize the bone regeneration, images obtained from a micro-computed tomography (CT) scanner (Skyscan 1173; Skyscan, Kontich, Belgium) were used, and the percentage of new bone formation within the defect was calculated using cross-sectional images obtained from the micro-CT data and ImageJ software (National Institutes of Health, Bethesda, MD). The area of new bone formation was determined by measuring the distance between the defect margin and new bone margin, and the percentage of new bone formation was calculated as the ratio of the new bone area to the total defect area. After micro-CT evaluation, the samples were embedded in paraffin, and were sectioned at 5 μm. The sections were stained with hematoxylin and eosin (H&E) and Masson's trichrome, and were observed under an optical microscope.

Statistical analysis

All experimental data ($n = 3$) are expressed as mean ± SD and were evaluated for significance by one-way analysis of variance (ANOVA) with a *post hoc* Tukey test using MINITAB (version 14.2; Minitab, Inc., State College, PA). Differences between experimental groups were considered statistically significant at $p < 0.05$.

Results

Ceramic scaffolds

Figure 1 shows the commercialized and fabricated ceramic scaffolds for the *in vitro* and *in vivo* tests. To fabricate the ceramic scaffolds, ceramic slurry (20%) was prepared and about 1.5-fold larger structures were designed to take into account the shrinkage of about 34% at maximum

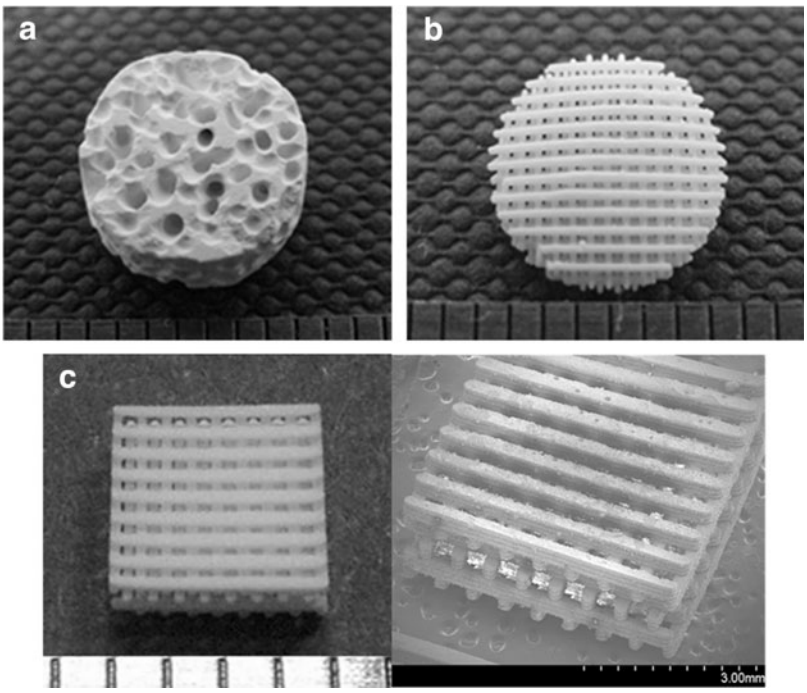

FIG. 1. Macroscopic and microscopic images showing the ceramic scaffolds used in this study: **(a)** commercialized HABI-HAP-PD, **(b, c)** fabricated ceramic scaffolds, **(a, b)** for *in vivo* experiments, and **(c)** for *in vitro* experiments.

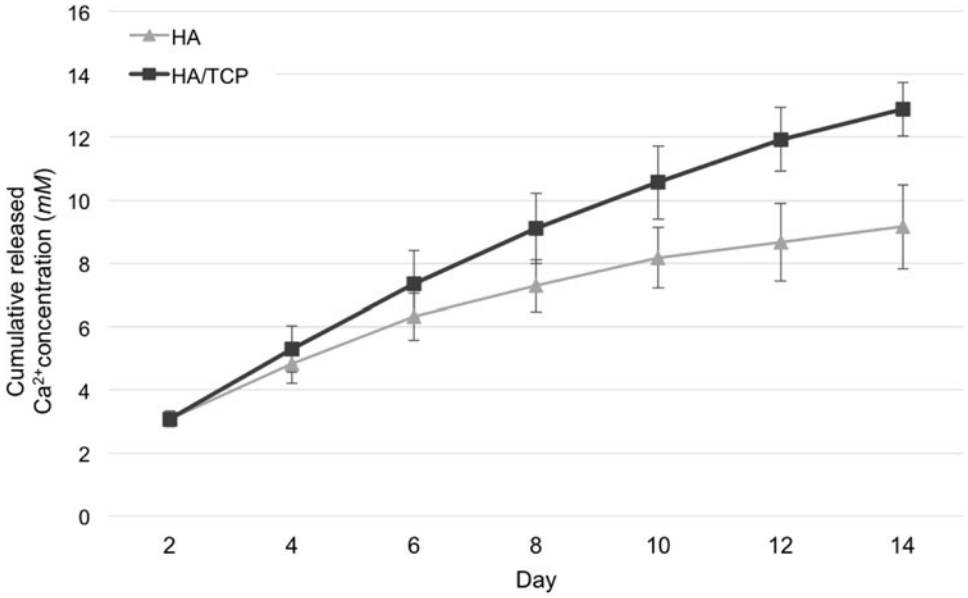

FIG. 2. Calcium ions release over the course of 14 days.

sintering temperature. We fabricated ceramic scaffolds with a staggered line arrangement. The pore size and line width of the scaffolds were about 300 μm. The dimensions of cuboid scaffold for the *in vitro* test were $3.9 \times 3.9 \times 2.8$ mm, and the cylindrical scaffold for the *in vivo* test was 8 mm in diameter and 1.5 mm in height. All of the pores in the fabricated scaffold were fully interconnected [Fig. 1(c)]. Moreover, gaps between ceramic particles generated naturally occurring pore sizes of 6.02 ± 1.19 and 3.47 ± 0.88 μm, for the HA and HA/TCP scaffolds respectively. The grain size of HA and HA/TCP scaffolds were 16.11 ± 1.4 and 9.95 ± 3.49 μm, respectively (Supplementary Fig. S1; Supplementary Data are available online at www.liebertpub.com/tea). These surface morphologies of ceramic scaffolds would facilitate cell adhesion, proliferation, and differentiation.[27–29]

Evaluation of calcium ion release

Figure 2 shows the results of a calcium ion release test using HA and HA/TCP scaffolds in the culture medium. HA/TCP scaffolds released more calcium ions than did HA scaffolds. At day 2, calcium concentration in growth medium containing HA/TCP and HA were similar, but calcium concentration increased faster over time in media containing HA/TCP (0.82 mM/day) than in those containing HA (0.51 mM/day). The HA/TCP scaffolds released more calcium ions than did the HA scaffolds because of the fast degradation of TCP. In both scaffolds, calcium ions were released continuously over the 14-day measurement period.

Biocompatibility of ceramic scaffolds

Cell proliferation was examined using DNA quantification. Because a ceramic scaffold is supposed to provide an environment that allows cellular proliferation and differentiation, the scaffold should not be toxic to cells. Figure 3 shows the results of the cell proliferation test. Cells on both HA and HA/TCP scaffolds proliferated well at the beginning of proliferation, but proliferation rate decreased as time passed. And, there were statistical differences between HA and HA/TCP scaffolds. Cells on HA scaffolds proliferated well compared to cells on HA/TCP scaffolds.

Osteogenic differentiation on ceramic scaffolds

ALP activity, AR-S staining, and RT-PCR were performed to validate the effects of calcium ions on osteogenic differentiation of cells. hTMSCs were cultured on HA and HA/TCP scaffolds in normal and osteogenic medium conditions. The results of ALP activity of cells cultured on HA and HA/TCP scaffolds for 7 days are shown in Supplementary Figure S2. Although there were no statistically significant differences between the HA and HA/TCP scaffolds, the ALP activity on the HA/TCP scaffolds was slightly higher than that on the HA scaffolds under both the conditions of normal and osteogenic medium. Figure 4 shows the images of AR-S staining of cells cultured on HA and HA/TCP scaffolds for 14 days. In this figure, the red color observed on the scaffolds indicates the presence of

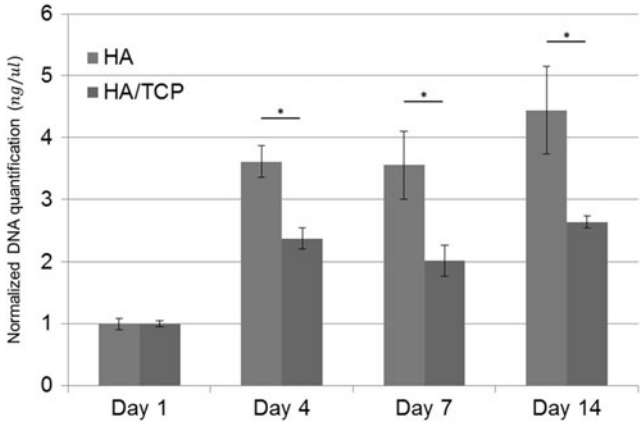

FIG. 3. Human turbinate mesenchymal stromal cell (hTMSC) proliferation on the ceramic scaffolds over the course of 14 days. $*p < 0.05$.

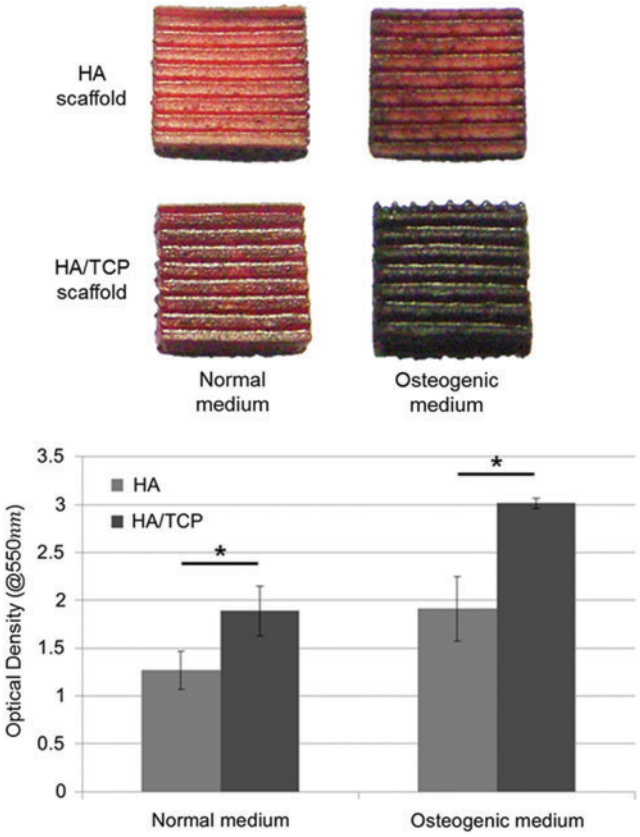

FIG. 4. Osteogenic differentiation of hTMSCs on ceramic scaffolds (Alizarin Red-S staining test). $*p < 0.05$. Color images available online at www.liebertpub.com/tea

calcium precipitation. The cells cultured on the HA/TCP scaffolds obviously showed a darker red color than the HA scaffolds. The results of the quantitative evaluation are shown in Figure 4. The optical density of the solutions extracted from the HA/TCP scaffolds was significantly higher than that from the HA scaffolds. Osteogenic differentiation was also characterized at the gene expression level as shown in Figure 5. HA/TCP scaffolds had a higher expression level of *OCN* than HA scaffolds, and statistically significant differences were observed under both types of medium conditions. The expression level of *Runx2* in the HA and HA/TCP scaffolds in normal medium did not differ significantly. However, in osteogenic medium, a significant difference was observed between the HA and HA/TCP scaffolds, in which the HA/TCP scaffolds had the higher expression level. For *Col-I*, like the expression level of *OCN*, the expression level in the HA/TCP scaffolds was higher than that in the HA scaffolds.

Analysis of new bone formation in vivo

To investigate the new bone formation capacity of the developed scaffolds *in vivo*, commercialized BABI-HAP-PD, HA scaffolds, and HA/TCP scaffolds were prepared and were implanted into rat calvarial defects. New bone formation in the implanted scaffolds was visualized using micro-CT as shown in the Figure 6. At 16 weeks after implantation, while newly generated bone tissue was easily observed in the HA and HA/TCP scaffolds, it was difficult to recognize the newly generated bone tissue in the blank and BABI-HAP-PD scaffolds. The quantitative analysis of new bone formation evaluated by ImageJ software is shown in Figure 7. The area of new bone formation in BABI-HAP-

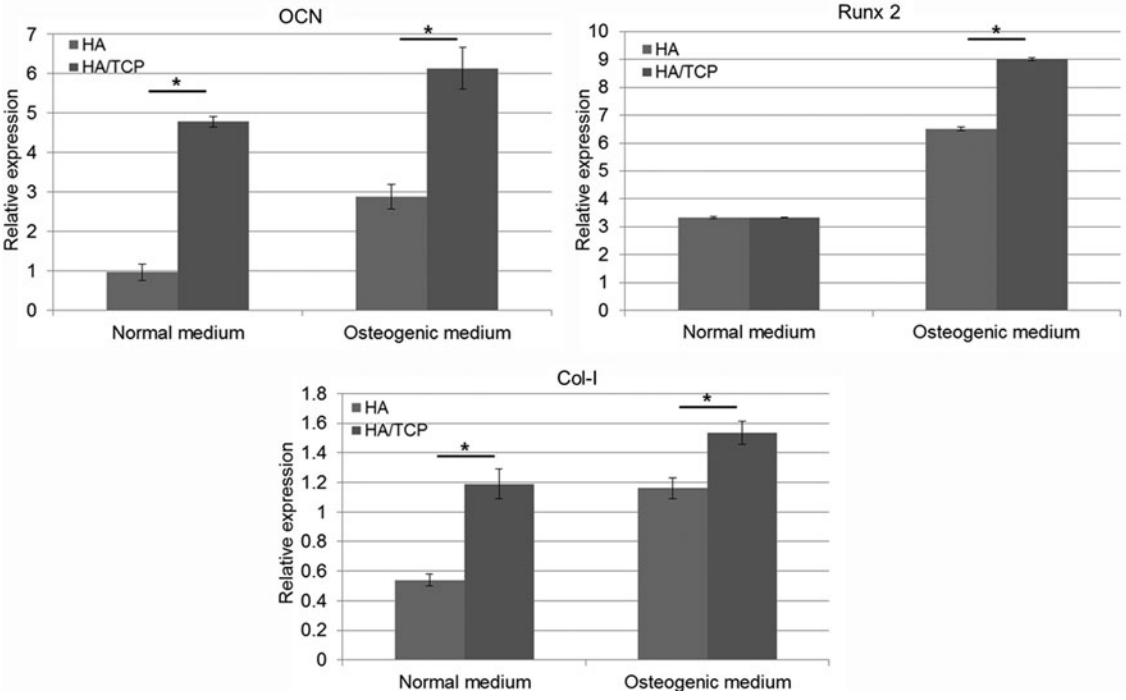

FIG. 5. Quantitative real-time reverse transcription–polymerase chain reaction gene expression analysis of osteogenic markers. $*p < 0.05$

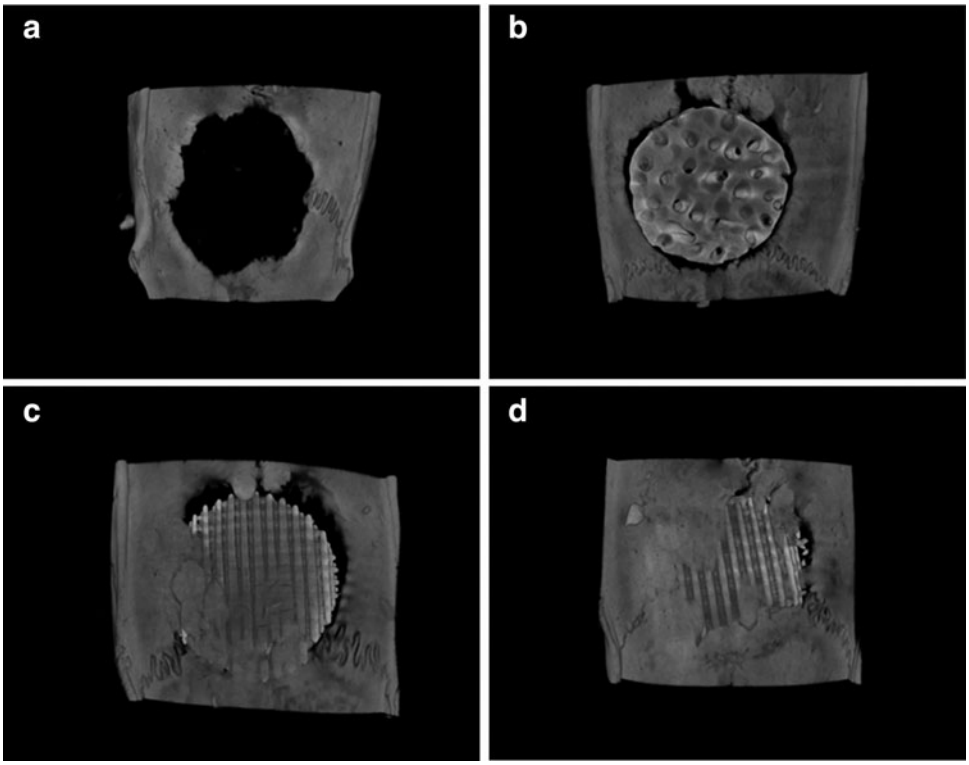

FIG. 6. Micro-computed tomography (CT) images showing new bone formation at the 16th week after implantation: **(a)** blank, **(b)** BABI-HAP-PD, **(c)** hydroxyapatite (HA), and **(d)** HA/tricalcium phosphate (TCP).

PD was similar to that in the blank group, and the area of new bone formation was about 7%. However, the area of new bone formation in the HA (29.34% ± 2.32%) and HA/TCP (54.83% ± 2.67%) scaffolds was higher than the blank group, while the best bone regeneration capacity was observed in the HA/TCP scaffolds.

Histological analysis

In a histological analysis using H&E, and Masson's trichrome staining at the 16th week after implantation, the results of histological staining showed a difference in the newly generated bone between BABI-HAP-PD and HA, and between HA and HA/TCP scaffolds, as shown in Figure 8. Newly generated bone was observed along the periphery of the defect and its extent was very limited in the blank group [Fig. 8(a, b)]. Because the BABI-HAP-PD scaffold had low porosity and thus did not have much space in which new bone could be generated, the newly generated bone was observed in the pores close to the defect [Fig. 8(c, d)]. In the HA and HA/TCP scaffolds, most of their pores were filled with cells and new bone was generated with continuity from the defect site to the inside of the scaffold [Fig. 8(e–h)]. However, in the HA/TCP scaffold, more bone tissue was generated, and the distance of the new bone ingrowth was longer than that in the HA scaffold.

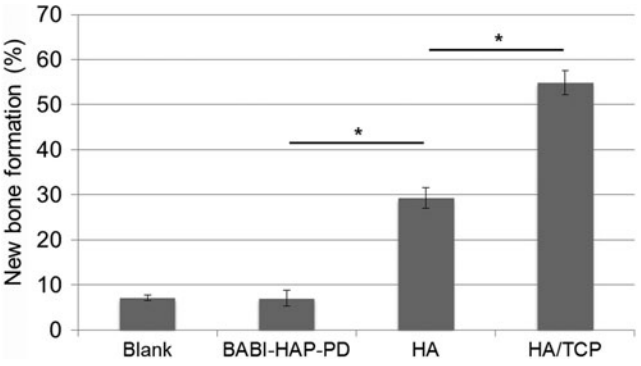

FIG. 7. New bone formation area at the 16th week after implantation. $*p < 0.05$.

Discussion

To fabricate the scaffold for bone tissue regeneration, ceramic materials such as HA and TCP were used. They are excellent materials for bone tissue regeneration; however, due to difficulties with their processability, they have usually been used as an additive or as a coating material to enhance bone regeneration.[30–33] Even when they have been used alone to fabricate bone scaffolds, most such scaffolds have been were fabricated by traditional methods and did not have full interconnectivity for bone tissue ingrowth.[34–36] To overcome these limitations, in this study, the pMSTL system, which is an AM technology, was applied and ceramic scaffolds with the desired shape and fully interconnected pores were successfully fabricated. The fabricated ceramic scaffolds maintained their regular pore size, and all of the pores in the ceramic scaffold were connected with one another. Furthermore, ceramic scaffolds fabricated in this study had porous and uneven surfaces, and HA/TCP scaffolds had smaller grain and micropore size compared with HA scaffolds (Supplementary Fig. S2). A porous and uneven surface can enhance cell adhesion and extracellular matrix (ECM) synthesis and mineralization.[27–29] Therefore, ceramic scaffolds fabricated in this study can enhance the ability to regenerate

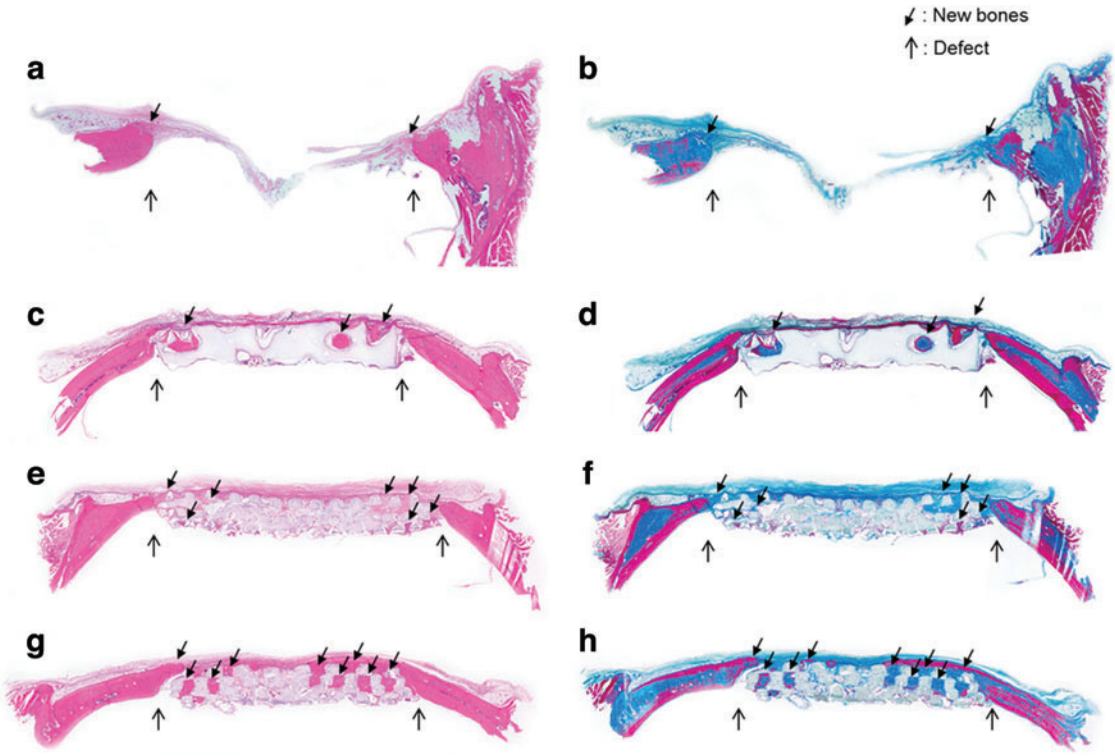

FIG. 8. The images (40×) of histological analysis using hematoxylin and eosin (H&E) **(a, c, e, g)** and Masson's trichrome **(b, d, f, h)** at the 16th week after implantation: **(a, b)** blank, **(c, d)** BABI-HAP-PD, **(e, f)** HA, and **(g, h)** HA/TCP. Color images available online at www.liebertpub.com/tea

bone tissue due to the surface characteristics. However, the roughness of HA and HA/TCP scaffolds could not be evaluated using atomic force microscopy (AFM) or a 3D surface profilometer, and compared, because these porous and uneven surfaces did not have an ideal surface to set as a baseline for measuring surface roughness.

Through the cell proliferation test, we demonstrated that the ceramic scaffolds did not show cytotoxicity and cell adhesion rate between HA and HA/TCP scaffold was similar. However, because osteogenic differentiation on the ceramic scaffolds was activated due to the calcium ions and surface morphology, cell proliferation rate decreased after 4 days (Fig. 3).

The HA and TCP materials used for scaffold fabrication degrade under *in vitro* and *in vivo* conditions, releasing calcium ions. It has been reported that the presence of extracellular calcium ions activates osteoblast chemotaxis and proliferation, and the osteogenic differentiation of stem cells. Moreover, calcium ions have been shown to stimulate osteoclast-medicated release of growth factors that enhance bone tissue remodeling.[8,11–15] In this study, to enhance the scaffold's capacity for regenerating bone tissue, scaffolds were fabricated from HA and TCP materials. Furthermore, the quantity of calcium ions released from the ceramic scaffold was adjusted by the composition of HA and TCP because the degradation rate of TCP is faster than that of HA. After fabricating the HA and HA/TCP scaffolds, energy dispersive X-ray analysis and X-ray diffraction spectrometry were conducted to compare elemental composition and to verify successful fabrication of HA and HA/TCP scaffolds (Supplementary Fig. S3). The results demonstrate that HA/TCP scaffolds consisted of HA and TCP, and crystalline phases of HA and TCP were detected in sintered HA/TCP scaffolds. The HA and HA/TCP scaffolds were successfully fabricated, and the quantity of calcium ions released from ceramic scaffolds was measured (Fig. 2). HA and TCP materials have different degradation rates, and as they degrade, they release calcium ions. Because calcium ions enhance the capacity for bone tissue regeneration, the quantity of calcium ions released from the ceramic scaffolds was measured using HA and HA/TCP scaffolds in the culture medium (Fig. 2). HA/TCP scaffolds released more calcium ions than did HA scaffolds. When we conducted *in vitro* experiments, the culture medium was changed every 3 days and the average concentration of calcium ions in the medium contacting HA/TCP scaffold was ~2.46 mM, and was higher than homeostatic range of calcium ions (1.1–1.3 mM) in the human body.[37] Consequently, the HA/TCP was able to provide an environment of higher concentration of calcium ions and would thus promote the regeneration of bone tissue.

Osteogenic differentiation tests were performed *in vitro* to determine the effects of calcium ions on bone tissue regeneration. In the results of osteogenic differentiation test using ceramic scaffolds, the ALP activity at day 7 on ceramic scaffolds did not show statistically significant differences between HA and HA/TCP scaffolds (Supplementary Fig. S3). ALP expresses at early stage of differentiation, and then expression decreases as time passed. The time point when ALP expression the highest was

closely related with experimental conditions and cell types. The highest ALP expression of HA/TCP scaffolds might have occurred at earlier than day 7. Therefore, there were no significant differences of ALP activity between HA and HA/TCP scaffolds at day 7. However, the result of AR-S staining showed that more mineralization occurred on HA/TCP scaffolds than HA scaffolds because calcium precipitation was deposited in the ECM over the *in vitro* culture period (Fig. 4). Like the results of ALP activity and AR-S staining, the results of RT-PCR showed that the expression of osteogenic genes, *OCN*, *Runx2*, and *Col-I*, were higher in cells cultured on the HA/TCP scaffolds than HA scaffolds. In the HA/TCP scaffolds, hTMSCs were differentiated to osteoblast-like cells more effectively. These were closely related with the results of the calcium ion release test. Additionally, we used exogenous calcium ions to verify their effects on osteogenic differentiation of cells in the cell culture dish without scaffolds. Cells cultured in the medium with exogenous calcium ions (2.46 mM) expressed higher levels of osteogenesis-related genes such as *OCN*, *Runx2*, and *Col-I* than the cells in the medium without exogenous calcium ions (Supplementary Fig. S4). This experiment demonstrated that elevated concentration of calcium ion promotes osteogenic differentiation of cells.

In the *in vivo* experiment, BABI-HAP-PD, HA, and HA/TCP scaffolds were implanted in rat calvarial defects, and bone tissue regeneration was evaluated using micro-CT images and histological assays. Unlike the *in vitro* experiments, commercialized BABI-HAP-PD scaffolds were added to compare the bone regeneration capacity of AM technology with that of the traditional method. The area of new bone formation in the HA scaffold was about fourfold higher than that in BABI-HAP-PD scaffold. The BABI-HAP-PD scaffolds had a few pores and they were not perfectly interconnected. This inner architecture made it difficult for bone tissue to regenerate effectively. Through these results, we confirmed that the interconnectivity of pores was a crucial factor for bone tissue regeneration. When we compared the HA and HA/TCP scaffolds, bone tissue was regenerated more extensively in the HA/TCP scaffolds, and these results were similar to the *in vitro* differentiation results. In the results of histological assay as shown in Figures 8 and 9, we could observe that bone tissue grew inside the scaffolds from the periphery of the defects, and most of the pores were filled with cells in both kinds of scaffold. Furthermore, Figure 9 shows that newly generated bone tissues integrated with the scaffolds, and they contained osteoblast-like cells, osteoclast-like cells, and osteocyte-like cells. In the HA/TCP scaffolds, more mature bone tissue was observed.

Through these experiments, we have demonstrated effect of calcium ion concentration and surface morphology in the ability of ceramic scaffolds to regenerate bone. HA/TCP scaffolds not only released higher quantity of calcium ions but also had smaller grain and pore size compared with the HA scaffolds, resulting in enhanced bone formation.

However, because ceramic materials, especially HA, have a slow degradation rate, it was difficult to recognize the degradation of the scaffolds over the course of just 16 weeks. Thus, to obtain a greater capacity for bone regeneration, further research on increasing the degradation rate of ceramic scaffolds is required.

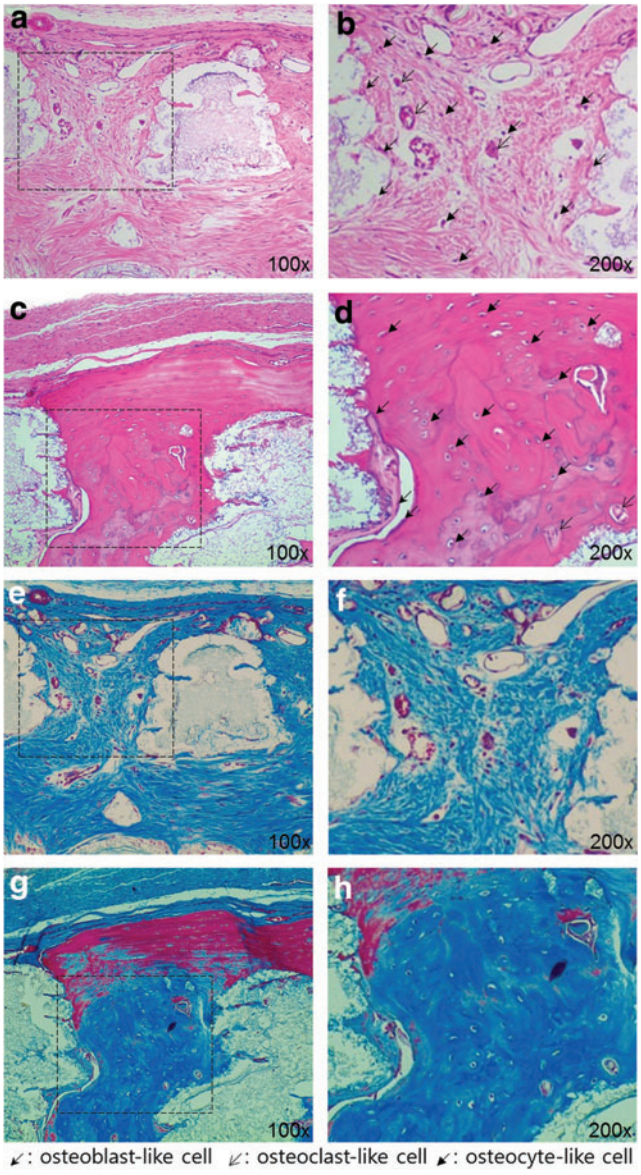

FIG. 9. Magnified images (100× and 200×) of histological assay using H&E **(a–d)** and Masson's trichrome **(e–h)** at the 16th week after implantation: **(a, b, e, f)** HA, and **(c, d, g, h)** HA/TCP. Color images available online at www.liebertpub.com/tea

Conclusions

In this study, we successfully fabricated a 3D ceramic scaffold using AM technology and demonstrated that the grain and micropore size of HA/TCP scaffolds were smaller than those of HA scaffolds. Also, we performed a calcium ion release test, and found that the quantity of calcium ions released from the scaffolds increased linearly, and the release occurred at a higher rate in the scaffolds including TCP. The effects of calcium ions on osteogenic differentiation and bone regeneration were evaluated *in vitro* and *in vivo*. Through these results, we have demonstrated that HA/TCP scaffolds had a greater capacity for bone regeneration than HA scaffolds, and that bone regeneration was enhanced by calcium releasing scaffolds with rough surface morphology. Moreover, we also have demonstrated that scaffolds

fabricated by AM technology were superior to scaffolds fabricated by traditional methods. The ceramic scaffolds developed in this study might be useful for enhancing the capacity of regeneration in complex bone defects.

Acknowledgments

This work was supported by the National Research Foundation of Korea (NRF) grant funded by the Korea Government (MEST & MSIP) (No. 2012-0001235, 2010-0018294, and 2011-0030075).

Disclosure Statement

No competing financial interests exist.

References

1. Einhorn, T.A. The cell and molecular biology of fracture healing. Clin Orthop Relat Res **355 Suppl,** S7, 1998.
2. Petite, H., Viateau, V., Bensaid, W., Meunier, A., de Pollak, C., Bourguignon, M., *et al.* Tissue-engineered bone regeneration. Nat Biotechnol **18,** 959, 2000.
3. Damien, C.J., and Parsons, J.R. Bone graft and bone graft substitutes: a review of current technology and applications. J Appl Biomater **2,** 187, 1991.
4. Hollister, S.J. Porous scaffold design for tissue engineering. Nat Mater **4,** 518, 2005.
5. Langer, R., and Vacanti, J.P. Tissue engineering. Science **260,** 920, 1993.
6. Giannobile, W.V. Periodontal tissue engineering by growth factors. Bone **19,** S23, 1996.
7. Stevens, M.M. Biomaterials for bone tissue engineering. Mater Today **11,** 18, 2008.
8. Place, E.S., Evans, N.D., and Stevens, M.M. Complexity in biomaterials for tissue engineering. Nat Mater **8,** 457, 2009.
9. Argintar, E., Edwards, S., and Delahay, J. Bone morphogenetic proteins in orthopaedic trauma surgery. Injury **42,** 730, 2011.
10. Dimitriou, R., Jones, E., McGonagle, D., and Giannoudis, P.V. Bone regeneration: current concepts and future directions. BMC Med **9,** 66, 2011.
11. Wen, L., Wang, Y., Wang, H., Kong, L., Zhang, L., Chen, X., *et al.* L-type calcium channels play a crucial role in the proliferation and osteogenic differentiation of bone marrow mesenchymal stem cells. Biochem Biophys Res Commun **424,** 439, 2012.
12. Gu, H.J., Guo, F.F., Zhou, X., Gong, L.L., Zhang, Y., Zhai, W.Y., *et al.* The stimulation of osteogenic differentiation of human adipose-derived stem cells by ionic products from akermanite dissolution via activation of the ERK pathway. Biomaterials **32,** 7023, 2011.
13. Titushkin, I., Sun, S., Shin, J., and Cho, M. Physicochemical control of adult stem cell differentiation: shedding light on potential molecular mechanisms. J Biomed Biotechnol **2010,** 14, 2010.
14. Jung, G.Y., Park, Y.J., and Han, J.S. Effects of HA released calcium ion on osteoblast differentiation. J Mater Sci Mater Med **21,** 1649, 2010.
15. Barradas, A.M.C., Fernandes, H.A.M., Groen, N., Chai, Y.C., Schrooten, J., van de Peppel, J., *et al.* A calcium-induced signaling cascade leading to osteogenic differentiation of human bone marrow-derived mesenchymal stromal cells. Biomaterials **33,** 3205, 2012.
16. Ohtsuki, C., Kamitakahara, M., and Miyazaki, T. Bioactive ceramic-based materials with designed reactivity for bone tissue regeneration. J R Soc Interface **6 Suppl 3,** S349, 2009.
17. Macchetta, A., Turner, I.G., and Bowen, C.R. Fabrication of HA/TCP scaffolds with a graded and porous structure using a camphene-based freeze-casting method. Acta Biomater **5,** 1319, 2009.
18. Hamadouche, M., and Sedel, L. Ceramics in orthopaedics. J Bone Joint Surg Br **82,** 1095, 2000.
19. Mooney, D.J., Mazzoni, C.L., Breuer, C., McNamara, K., Hern, D., Vacanti, J.P., *et al.* Stabilized polyglycolic acid fibre-based tubes for tissue engineering. Biomaterials **17,** 115, 1996.
20. Lo, H., Ponticiello, M.S., and Leong, K.W. Fabrication of controlled release biodegradable foams by phase separation. Tissue Eng **1,** 15, 1995.
21. Peltola, S.M., Melchels, F.P., Grijpma, D.W., and Kellomaki, M. A review of rapid prototyping techniques for tissue engineering purposes. Ann Med **40,** 268, 2008.
22. Seol, Y.J., Kang, T.Y., and Cho, D.W. Solid freeform fabrication technology applied to tissue engineering with various biomaterials. Soft Matter **8,** 1730, 2012.
23. Shor, L., Guceri, S., Wen, X.J., Gandhi, M., and Sun, W. Fabrication of three-dimensional polycaprolactone/hydroxyapatite tissue scaffolds and osteoblast-scaffold interactions *in vitro*. Biomaterials **28,** 5291, 2007.
24. Jung, J.W., Kang, H.W., Kang, T.Y., Park, J.H., Park, J., and Cho, D.W. Projection image-generation algorithm for fabrication of a complex structure using projection-based microstereolithography. Int J Precis Eng Manuf **13,** 445, 2012.
25. Kim, J., Lim, D., Kim, Y., Young-Hag, K., Lee, M., Han, I., *et al.* A comparative study of the physical and mechanical properties of porous hydroxyapatite scaffolds fabricated by solid freeform fabrication and polymer replication method. Int J Precis Eng Manuf **12,** 695, 2011.
26. Sohn, Y.S., Jung, JW., Kim, J.Y., and Cho, D.W. Investigation of bi-pore scaffold based on the cell behaviors on 3D scaffold patterns. Tissue Eng Regen Med **8,** 66, 2011.
27. Boyan, B.D., Hummert, T.W., Dean, D.D., and Schwartz, Z. Role of material surfaces in regulating bone and cartilage cell response. Biomaterials **17,** 137, 1996.
28. Deligianni, D.D., Katsala, N.D., Koutsoukos, P.G., and Missirlis, Y.F. Effect of surface roughness of hydroxyapatite on human bone marrow cell adhesion, proliferation, differentiation and detachment strength. Biomaterials **22,** 87, 2001.
29. Yuan, H.P., Fernandes, H., Habibovic, P., de Boer, J., Barradas, A.M.C., de Ruiter, A., *et al.* Osteoinductive ceramics as a synthetic alternative to autologous bone grafting. Proc Natl Acad Sci U S A **107,** 13614, 2010.
30. Neuendorf, R.E., Saiz, E., Tomsia, A.P., and Ritchie, R.O. Adhesion between biodegradable polymers and hydroxyapatite: relevance to synthetic bone-like materials and tissue engineering scaffolds. Acta Biomater **4,** 1288, 2008.
31. McCullen, SD., Zhu, Y., Bernacki, S.H., Narayan, R.J., Pourdeyhimi, B., Gorga, R.E., *et al.* Electrospun composite poly(L-lactic acid)/tricalcium phosphate scaffolds induce proliferation and osteogenic differentiation of human adipose-derived stem cells. Biomed Mater **4,** 035002, 2009.
32. Lickorish, D., Ramshaw, J.A.M., Werkmeister, J.A., Glattauer, V., and Howlett, C.R. Collagen-hydroxyapatite composite prepared by biomimetic process. J Biomed Mater Res A **68A,** 19, 2004.

33. Lan, P.X., Lee, J.W., Seol, Y.J., and Cho, D.W. Development of 3D PPF/DEF scaffolds using micro-stereolithography and surface modification. J Mater Sci-Mater Med **20,** 271, 2009.
34. Deville, S., Saiz, E., and Tomsia, A.P. Freeze casting of hydroxyapatite scaffolds for bone tissue engineering. Biomaterials **27,** 5480, 2006.
35. Kandel, R.A., Grynpas, M., Pilliar, R., Lee, J., Wang, J., Waldman, S., *et al.* Repair of osteochondral defects with biphasic cartilage-calcium polyphosphate constructs in a Sheep model. Biomaterials **27,** 4120, 2006.
36. Ramay, H.R.R., and Zhang, M. Biphasic calcium phosphate nanocomposite porous scaffolds for load-bearing bone tissue engineering. Biomaterials **25,** 5171, 2004.
37. Dvorak, M.M., and Riccardi, D. Ca2+ as an extracellular signal in bone. Cell Calcium **35,** 249, 2004.

Address correspondence to:
Dong-Woo Cho, PhD
Department of Mechanical Engineering
Center for Rapid Prototyping Based 3D Tissue/Organ Printing
Pohang University of Science and Technology (POSTECH)
San 31 Hyoja-Dong, Nam-Gu
Gyungbuk
Pohang 790-784
Korea

E-mail: dwcho@postech.ac.kr

Received: December 7, 2012
Accepted: April 16, 2014
Online Publication Date: June 23, 2014